Palaeogeography, Palaeoclimatology, Palaeoecology 363–364 (2012) 23–36

Contents lists available at SciVerse ScienceDirect

Palaeogeography, Palaeoclimatology, Palaeoecology

journal homepage: www.elsevier.com/locate/palaeo

Vegetation and climatic changes of SW China in response to the uplift of Tibetan Plateau

Qian-Qian Zhang [a,b], David K. Ferguson [c], Volker Mosbrugger [d], Yu-Fei Wang [a], Cheng-Sen Li [a,*]

[a] State Key Laboratory of Systematic and Evolutionary Botany, Institute of Botany, Chinese Academy of Sciences, Xiangshan, Beijing, 100093, PR China
[b] Graduate University of the Chinese Academy of Sciences, Beijing, 100039, PR China
[c] Institute of Palaeontology, University of Vienna, Althanstrasse 14, Vienna A-1090, Austria
[d] Senckenberg Research Institute and Natural History Museum, Senckenberganlage 25, 60325, Frankfurt, Germany

ARTICLE INFO

Article history:
Received 25 November 2011
Received in revised form 23 August 2012
Accepted 24 August 2012
Available online 7 September 2012

Keywords:
Palaeovegetation
Climatic changes
Asian monsoon
Tibetan Plateau
Middle Miocene
SW China

ABSTRACT

To understand the vegetation succession and climatic changes at the southeastern margin of the Tibetan Plateau in the Neogene, we reconstructed the Middle Miocene vegetation and climate based on palynological data from four localities, which are at different latitudes along the Ailao Mountains in Yunnan, southwest China. The palynological assemblages suggest that the vegetation there was composed of mixed evergreen and deciduous broad-leaved forests growing under subtropical conditions. Based on the palynological data, the palaeoclimatic parameters from the four localities are established. The new parameters were compared with those of the Late Miocene, of the Late Pliocene, and of today. The comparison revealed that the temperatures were obviously lower in the Middle Miocene than they are today. This suggested that the Ailao Mountains were not high enough to block the Asian Winter Monsoon in the Middle Miocene. The Middle Miocene vegetation at the southeastern edge of the Tibetan Plateau was also compared to that of Central Tibet. It would appear that the palaeoclimate at the southeastern edge of the Tibetan Plateau was warmer and wetter than in Central Tibet. In contrast to the Neogene cooling in Central Europe, the climate at the southeastern edge of the Tibetan Plateau has gradually warmed since the Middle Miocene. This phenomenon was most likely caused by the uplift of the Tibetan Plateau, which has succeeded in blocking the Asian Winter Monsoon since the Middle Miocene.

1. Introduction

During the Neogene, the global climate was characterised by a general cooling trend (Zachos et al., 2001; Mosbrugger et al., 2005). The ecosystem dramatically changed in Asia due to the collision of the Indian and Asian continental plates (Mulch and Chamberlain, 2006). The uplift of the Tibetan Plateau not only caused changes in the regional landforms, the climate and the biodiversity of China (Li and Fang, 1998; Kou et al., 2006), but also profoundly influenced the development of the Asian monsoons (Li, 1999; An et al., 2001, 2006). The East Asian Monsoon was established approximately at the Oligocene/Miocene boundary and experienced three times of intensification at approximately 15–13 Ma, 8 Ma and 3 Ma (Sun and Wang, 2005).

A large number of investigations have explored the Neogene climatic changes in North America (e.g., Wolfe, 1994, 1995; Retallack, 2007), Northern Australia (e.g., Kershaw and Wagstaff, 2001; Kershaw et al., 2007) and Europe (e.g., Mosbrugger et al., 2005; Böhme et al., 2007; Uhl et al., 2007; Utescher et al., 2009).

In China, quantitative reconstructions of the Neogene climate have been made in recent years (e.g., Yang et al., 2002; Liang et al., 2003; Hao et al., 2010; Qin et al., 2011). More work combining the Neogene vegetation and the climatic changes in China must be designed and carried out, especially with respect to the Tibetan Plateau and its surrounding areas. In this study, the fossil plants found in the central and southern regions of Yunnan were examined to help understand the Neogene climatic changes in SW China. Yunnan (97°39′–106°12′ E,21°9′–29°15′N) is located on the southeastern edge of the Tibetan Plateau, and its climate is influenced by the Asian monsoons (Fig. 1a). It is widely accepted that the uplift of the Tibetan Plateau caused changes in the topography of Yunnan (BGMRYP, 1990; Zhang et al., 1997; Mulch and Chamberlain, 2006). The special geographical position and the abundant floral resources make Yunnan one of the most important regions for studying the climatic changes caused by the phased upheaval of the Tibetan Plateau (WGCPC, 1978; Xu et al., 2008; Xia et al., 2009).

The investigations of the Cenozoic mega-fossils from the Yunnan can be traced back to the early 20th century (Colani, 1920), with approximately 10 mega-floras having been documented: Oligocene floras (WGCPC, 1978), Miocene floras (WGCPC, 1978; Tao and Du, 1982; Tao and Chen, 1983; Zhao et al., 2004; Xia et al., 2009) and Pliocene floras (Tao and Kong, 1973; Tao, 1986; Sun et al., 2003; Dai et

* Corresponding author. Tel.: +86 10 6283 6436; fax: +86 10 6259 3385.
E-mail address: lics@ibcas.ac.cn (C.-S. Li).

0031-0182/$ – see front matter © 2012 Elsevier B.V. All rights reserved.
http://dx.doi.org/10.1016/j.palaeo.2012.08.009

al., 2009; N. Li et al., 2009). The Cenozoic palynofloras of Yunnan include Paleogene floras (Song and Li, 1976; Song and Zhong, 1984) and Neogene floras (Li and Wu, 1978; Sun and Wu, 1980; Song, 1988; Hou and Li, 1993; Wang, 1996; Zhang et al., 1996; Xu et al., 2003; Wang and Shu, 2004; Kou et al., 2006; Xu et al., 2008). Quantitative reconstructions of the Neogene climate in Yunnan have been carried out in recent years (Zhao et al., 2004; Kou et al., 2006; Xu et al., 2008; Xia et al., 2009).

The present research attempts to detect the signals of the East Asian Monsoon on the southeastern edge of the Tibetan Plateau in the Middle Miocene, to explore the Neogene climatic changes in SW China and to evaluate the intercontinental climatic differences. Here, we studied the spores and pollen from four coal mines of the Middle Miocene age, and we reconstructed the paleoclimates quantitatively. These coal mines are located in Cenozoic coal-bearing basins in the central and southern parts of Yunnan. Based on the palynological data, we determined that the vegetation in these basins changed from the north to the south, with an increase of angiospermous elements and a decrease in gymnosperms and ferns. By using the Coexistence Approach (Mosbrugger and Utescher, 1997), we obtained the Middle Miocene climatic parameters in all four basins. The results suggested that the climate in the Middle Miocene of Yunnan was cooler than that of today. This may have been caused by the uplift of the Tibetan Plateau as well as by the Asian Winter Monsoon (BGMRYP, 1990; Zhang et al., 1997; Kou et al., 2006).

2. Materials and methods

2.1. Study site

The four coal-mines are located in Cenozoic coal-bearing basins in the central and southern parts of Yunnan. From north to south, they are the Dajie coal mine in Jingdong County (DJ), the Hexi coal mine in Zhenyuan County (HX), the Pojiao coal mine in Puwen Town (PJ) and the Shanggang coal mine in Mengla County (SG) (Fig. 1b).

2.1.1. The DJ coal mine

The DJ opencast coal mine (24°19′25.3″N, 101°03′31.2″E, 1328 ± 10 m a.s.l.) lies approximately 23 km south of Jingdong County, Yunnan Province. The sediments in the coal-mine belong to the Dajie Formation and are Miocene in age (Ge and Li, 1999). The Dajie Formation in this area is between 285 and 733 m thick (Ge and Li, 1999), whereas the sediments of the DJ section are only 31.9 m thick (Fig. 2a). By comparing against the lithostratigraphic characters of the Dajie Formation, it has been suggested that the DJ section belongs to the middle portion of the Dajie Formation. The section is overlain by Quaternary sediments, but the underlying sediments remain unidentified. The exposure consists of 11 layers, from which 57 palynological samples were collected. The samples were taken from the mudstone and lignite (Fig. 2a). The lithostratigraphic characters of the section are described as follows:

Overlying strata: Quaternary sediment	
Unconformity	
11 Thin layers of coal and light grey mudstone	5 m
10 Thick layers of light grey mudstone with thin layers of sandstone	10 m
9 Thin layers of coal with light gray mudstone	1 m
8 Thick layers of yellow-green mudstone and silty mudstone	2.5 m
7 Light grey mudstone with three layers of coal at the top, middle and bottom, each measuring 10–15 cm thick	2 m
6 Thick layers of light grey mudstone	1.1 m
5 Coal with thin layers of light grey mudstone	2 m
4 Thick layers of light grey mudstone and silty mudstone	4.3 m
3 Thin layers of coal and thin layers of light grey carbonaceous mudstone	2 m
2 Coal	1 m
1 Black mudstone	1 m
Bottom unidentified	

2.1.2. The HX coal mine

The HX coal mine (23°35′10.2″N, 101°09′43.5″E, 980 m a.s.l.) is located at about approximately 57 km south of the city of Zhenyuan. The sediments in the coal-mine also belong to the Dajie Formation (Ge and Li, 1999). The Dajie Formation in this area is 137–735 m thick (Ge and Li, 1999), while the sediments of the HX section exposed here are only 70 m thick. By comparing against the lithostratigraphic characters of the Dajie Formation, it has been suggested that the HX section belongs to the middle portion of the Dajie Formation The section is overlain by Quaternary sandy conglomeratic sediments and is underlain by light grey mudstone. The section consists of 14 layers. Fifty-three palynological samples were collected from these layers. The samples were taken from the mudstone and lignite (Fig. 2b). The lithostratigraphic characters of the section are described as follows:

Overlying strata: Quaternary sandy conglomeratic sediment	
Unconformity	
14 Coal with thin layers of mudstone at the top	3.5 m
13 Thick layers of light grey mudstone with thin layers of carbonaceous mudstone	12 m
12 Thick layers of brick-red mudstone	5 m
11 Thin layers of light grey mudstone and coal	6 m
10 Thick layers of light grey mudstone with coal of 5–10 cm thick in the middle portion (with leaves present)	5 m
9 Coal with thin layers of light grey mudstone	3 m
8 Thick layers of light grey mudstone and a small amount of silty mudstone	9 m
7 Light grey mudstone with carbonaceous mudstone of 20 cm thick at the bottom	4 m
6 Light grey mudstone	4.5 m
5 Mudstone with thin layers of coal	6 m
4 Thick layers of light grey mudstone and thin layers of silty mudstone	8 m
3 Thin layers of light yellow mudstone, silty mudstone and thin layers of coal	1.5 m
2 Coal	2.5 m
1 Thick light grey mudstone	
Bottom unidentified	

2.1.3. The PJ coal mine

The PJ coal mine is exposed at Puwen Town, Jinghong City in Yunnan Province. By comparing against the lithostratigraphic characters of the Dajie Formation, it has been suggested that the sediments of the coal-mine also belong to the middle portion of the Dajie Formation (Zheng et al., 1976; Ge and Li, 1999). Seven palynological samples were collected from seven bore cores, viz. PJ1 (22°27′44.5″N, 101°03′44.8″E, 881 ± 8 m a.s.l.), PJ2 (22°27′45.7″N, 101°03′45.7″E, 887 ± 8 m a.s.l.), PJ3 (22°27′46.1″N, 101°03′40.0″E, 898 ± 9 m a.s.l.), PJ4 (22°27′46.3″N, 101°03′41.2″E, 886 ± 9 m a.s.l.), PJ5 (22°27′42.5″N, 101°03′44.3″E, 884 ± 8 m a.s.l.), PJ6 (22°27′42.5″N, 101°03′46.1″E, 884 ± 7 m a.s.l.), PJ7 (22°27′40.7″N, 101°03′44.3″E, 884 ± 7 m a.s.l.). The samples were taken from the mudstone and lignite.

2.1.4. The SG coal mine

The SG coal mine (21°17′05.9″N, 101°41′22.3″E, 764 ± 7 m a.s.l.) is located in Mengla County, near the Sino-Laotian border. By comparing with the lithostratigraphic characters of the Dajie Formation, it has been suggested that the sediments of the coal-mine also belong to the middle portion of the Dajie Formation (Ge and Li, 1999). We collected 10 palynological samples here. The samples were taken from the lignite.

2.2. Methods

The palynological samples were analysed by the heavy liquid separation method (density = 2.0 g/ml) (Moore et al., 1991; Li and Du, 1999). The pollen grains and spores were observed under a Leica DM 2500 microscope (Fig. 3), and more than 16,800 palynomorphs were identified with the data from the literature (IBCAS, 1976; Zhang et al., 1976; IBCAS and SCIBCAS, 1982; Wang et al., 1995). The single-grain technique (Ferguson et al., 2007) was applied to show the good quality of images by using an FEI Quanta 200 environmental scanning electron microscope (Figs. 4, 5).

In this work, the palynomorph taxa were grouped according to the temperature requirements of their nearest living relatives (Jiménez-Moreno, 2006; J.F. Li et al., 2009; Qin et al., 2011). We use the Coexistence Approach (CA; Mosbrugger and Utescher, 1997) for the quantitative reconstruction of the Middle Miocene climate. The basic principle of CA is the assumption that the climatic requirement of a fossil taxon is similar to that of its Nearest Living Relative (NLR). Based on the geographic distributions of all NLRs (Wu and Ding, 1999), the climatic parameters and coexistence intervals of the fossil taxa in a palynoflora are obtained. The modern climatic parameters of NLRs used in CA are extracted from the surface meteorological data of China (average value of 30 years from 1951 to 1980) (IDBMC, 1984). Meanwhile, the MAT values of NLRs from the Palaeoflora Database were also adopted to obtain the seven climatic parameters (http://www.palaeoflora.de/). These are: MAT = the mean annual temperature, MWMT = the mean temperature of the warmest month, MCMT = the mean temperature of the coldest month, DT = the difference in temperature between the coldest and warmest months, MAP = the mean annual precipitation, MMaP = the mean maximum monthly precipitation, and MMiP = the mean minimum monthly precipitation.

3. Results

3.1. Palynological assemblages

3.1.1. The DJ palynological assemblages

In the DJ section, the 60 palynomorphs consist of 37 angiosperms (belonging to 31 families and accounting for 30.51% of the total number of pollen and spores), nine gymnosperms (five families/12.06%), 13 pteridophytes (12 families/57.39%) and an alga (one family of Zygnemataceae /0.04%) (Fig. 6a, Table S1).

Three megathermic elements (Rutaceae, Sapindaceae and Symplocaceae), seven mega-mesothermic elements (Taxodiaceae, *Castanopsis*, *Ilex*, Hamamelidaceae, Araliaceae, Anacardiaceae and Myrtaceae), 16 mesothermic elements (e.g., *Ginkgo*, *Alnus*, *Betula*, *Corylus*, *Quercus*), two meso-microthermic elements (*Pinus* and *Tsuga*), and two microthermic elements (*Abies* and *Picea*), were recorded.

The palynological assemblage is divided into three zones from the bottom to the top (Fig. 6a):

Zone 1 (sample numbers DJ1–DJ23) The 39 palynomorphs in Zone 1 include 24 angiosperm taxa (20 families), seven gymnosperms (four families) and eight pteridophytes (seven families). This zone is characterised by the dominance of pteridophytic spores, with an average value of 59.36% of the total number of pollen and spores, including Polypodiaceae (43.45%), *Pteris* (10.94%), *Athyrium* (2.42%) and Hemionitidaceae (1.77%). The angiosperm pollen (30.45%) is dominated by *Castanopsis* (17.42%) and *Alnus* (10.09%). The gymnosperm pollen (10.18%) consists mainly of *Pinus* (9.72%).

In this zone, two megathermic elements (Rutaceae and Sapindaceae), four mega-mesothermic elements (Taxodiaceae, *Ilex*, *Castanopsis* and Hamamelidaceae), 15 mesothermic elements (e.g., *Ginkgo*, *Alnus*, *Betula*, *Corylus*, *Quercus*), two meso-microthermic elements (*Pinus* and *Tsuga*), and two microthermic elements (*Abies* and *Picea*), are detected (Table S1).

Zone 2 (sample numbers DJ24–DJ34) In Zone 2, the 31 sporomorphs comprise 21 angiosperms (18 families), five gymnosperms (three families) and five pteridophytes (five families). Compared with Zone 1, the percentages of pteridophytic spores (44.38%) decreased, while those of angiosperm pollen (37.94%) and gymnosperm pollen (17.68%) increased. The angiosperms are still dominated by *Alnus* (25.74%) and *Castanopsis* (7.78%). The gymnosperm pollen is mainly represented by *Pinus* (16.52%). As one of the most common pteridophytes, the spores of Polypodiaceae occur in a frequency of 29.78%, which is lower than that (43.45%) of Zone 1 (Table S1).

Two megathermic elements (Rutaceae and Sapindaceae), four mega-mesothermic elements (*Castanopsis*, Araliaceae, Anacardiaceae and Hamamelidaceae), 10 mesothermic elements (e.g., *Alnus*, *Betula*, *Juglans*), two meso-microthermic elements (*Pinus* and *Tsuga*), and only one microthermic element (*Abies*), are present in this zone (Table S1).

Zone 3 (sample numbers DJ35–DJ57) In Zone 3, the 38 palynomorphs include 22 angiosperms (19 families), five gymnosperms (four families), 11 pteridophytes (10 families) and an alga (Zygnemataceae). Pteridophytic spores still predominate in this zone and reach an average value of 65.01%. Angiosperm and gymnosperm pollen respectively represent 22.82% and 11.97%, and both are less common than in Zone 2 (Table S1).

Three megathermic elements (Rutaceae, Sapindaceae and Symplocaceae), five mega-mesothermic elements (Taxodiaceae, Myrtaceae, *Ilex*, *Castanopsis* and Araliaceae), 11 mesothermic elements (e.g., *Alnus*, *Betula*, *Corylus*), two meso-microthermic elements (*Pinus* and *Tsuga*) are detected in this zone, but no microthermic elements are present.

3.1.2. The HX palynological assemblages

In the HX section, the 45 palynomorphs consist of 31 angiosperms (belonging to 23 families and accounting for 45.91% of the total number of pollen and spores), four gymnosperms (two families/8.77%), and 10 pteridophytes (nine families/45.32%) (Fig. 6b, Table S2).

Two megathermic elements (Meliaceae and Sapindaceae), six mega-mesothermic elements (*Ilex*, *Castanopsis*, Myrtaceae, Araliaceae, Hamamelidaceae and Anacardiaceae), 19 mesothermic elements (e.g., *Alnus*, *Betula*, *Corylus*, *Quercus*), two meso-microthermic elements (*Pinus* and *Tsuga*), and one microthermic element (*Abies*) is present.

The palynological assemblage is divided into five zones from the bottom to the top (Fig. 6b):

Zone 1 (sample numbers HX1–HX10) In Zone 1, there are 23 palynomorphs consisting of 15 angiosperms (52.5%), four gymnosperms (9.33%) and four pteridophytes (38.17%) (Table S2). Angiosperms belonging to 10 families dominate in this zone, the most important of which are *Castanopsis* (28.75%), *Alnus* (12%) and Fagaceae (7.08%). Gymnosperms are represented by *Pinus* (8.5%), *Tsuga* (0.42%), *Ephedra* (0.33%) and *Abies* (0.08%). Pteridophytic spores mainly belong to the Polypodiaceae (30.42%) and *Pteris* (6.42%).

In this zone, only one megathermic element (Meliaceae), two mega-mesothermic elements (*Ilex* and *Castanopsis*), nine mesothermic elements (e.g., *Alnus*, *Betula*), two meso-microthermic elements (*Pinus* and *Tsuga*), and one microthermic element (*Abies*) are present.

Zone 2 (sample numbers HX11–HX18) In Zone 2, the 18 palynomorphs comprise 10 angiosperms (six families), three gymnosperms (two families) and five pteridophytes (five families) (Table S2). The angiosperm pollen still dominates in this zone and reaches up to 65.59%. However, *Alnus* (45.02%) replaces *Castanopsis* (16.08%) as the most common angiosperm. *Pinus* (4.18%) is present at a lower frequency than in Zone 1. The pteridophytic spores are dominated by *Polypodium* (21.97%), *Athyrium* (4.29%) and *Pteris* (2.89%).

There is no megathermic element. However, there are three mega-mesothermic elements (*Ilex*, *Castanopsis* and Myrtaceae), six mesothermic elements (e.g., *Alnus*, *Betula*), two meso-microthermic elements (*Pinus* and *Tsuga*), but no microthermic element in this zone.

Zone 3 (sample numbers HX19–HX31) In Zone 3, the 27 palynomorphs consist of 16 angiosperms (13 families), four gymnosperms (two families) and seven pteridophytes (six families). Compared with Zone 2, the percentage of angiosperm pollen (51.03%) decreased, but gymnosperm pollen (19.29%) increased. *Castanopsis* (40.06%) and *Alnus* (7.87%) continue to dominate in this zone. *Pinus*

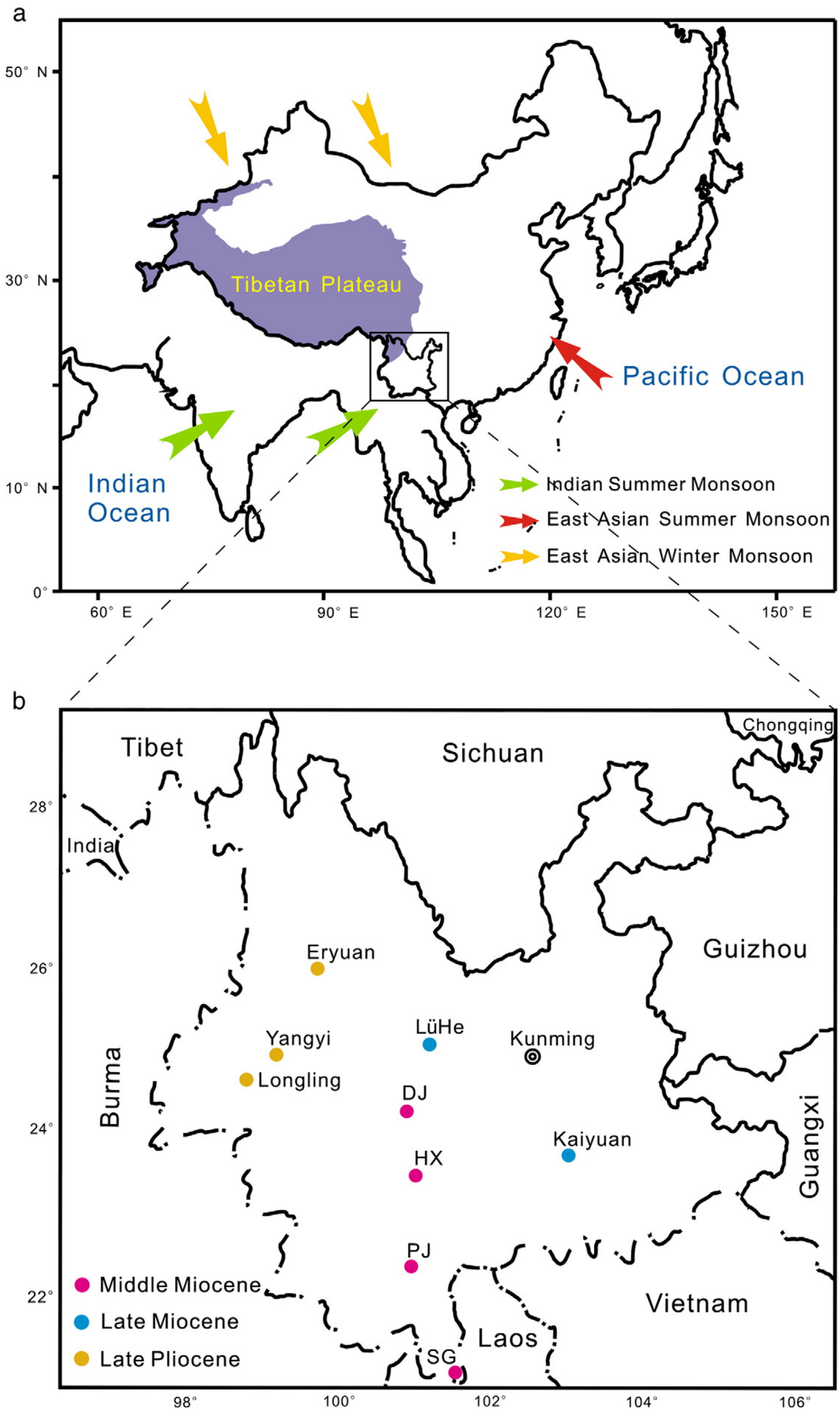
a
50° N
30° N
10° N
0°
60° E
90° E
120° E
150° E
Tibetan Plateau
Pacific Ocean
Indian Ocean
Indian Summer Monsoon
East Asian Summer Monsoon
East Asian Winter Monsoon
b
Tibet
Sichuan
Chongqing
India
Guizhou
Eryuan
LüHe
Kunming
Yangyi
Longling
Burma
DJ
Kaiyuan
HX
Guangxi
PJ
Middle Miocene
Late Miocene
Late Pliocene
Vietnam
Laos
SG
28°
26°
24°
22°
98°
100°
102°
104°
106°

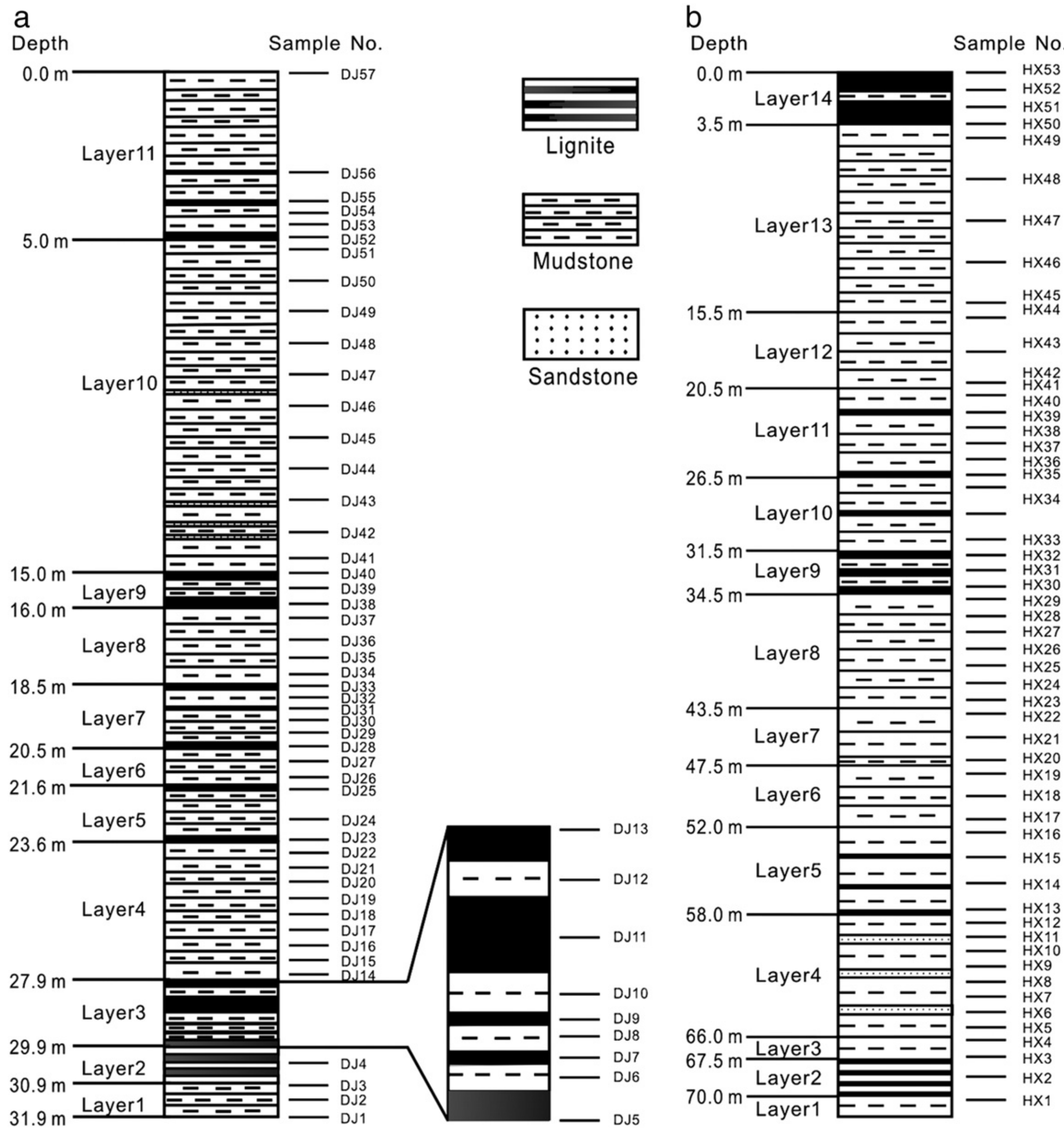

Fig. 2. The measured stratigraphic sequences of the section. a. DJ. b. HX.

(16.04%) and *Tsuga* (3.05%) are present at higher frequencies in this zone than in either Zones 1 or 2 (Table S2).

In Zone 3, one megathermic element (Sapindaceae), three mega-mesothermic elements (*Ilex*, *Castanopsis* and Myrtaceae), eight mesothermic elements (e.g., *Alnus*, *Betula*), two meso-microthermic elements (*Pinus* and *Tsuga*), and one microthermic element (*Abies*) is discovered.

Zone 4 (sample numbers HX32–HX46) In Zone 4, the 29 palynomorphs consist of 16 angiosperms (13 families), four gymnosperms (two families) and nine pteridophytes (eight families). This zone is characterised by the dominance of pteridophytic spores, with an average value of 67.16% of the total number of pollen and spores, including Polypodiaceae (43.90%) and *Pteris* (20.40%). Angiosperms (29.28%) are dominated by *Castanopsis* (14.06%) and *Alnus* (13.59%). The gymnosperm pollen (3.57%) is represented mainly by *Pinus* (2.46%) and *Tsuga* (0.91%).

One megathermic element (Sapindaceae), five mega-mesothermic elements (*Ilex*, *Castanopsis*, Araliaceae, Hamamelidaceae and Anacardiaceae), eight mesothermic elements (e.g., *Alnus*, *Corylus*), two meso-microthermic elements (*Pinus* and *Tsuga*), and one microthermic element (*Abies*) is found in this zone (Table S2).

Zone 5 (sample numbers HX47–HX53) In Zone 5, the 28 palynomorphs belong to 17 angiosperms (13 families representing 49.29% of the total number of pollen and spores), three gymnosperms (two families/5.40%), and eight pteridophytes (seven families/45.31%). Compared with Zone 4, the angiosperms, which replace the pteridophytes, again dominate in the assemblage. The percentage of *Alnus* (28.86%) is higher (13.59%) than in Zone 4 (Table S2).

Fig. 1. Maps showing the position of the study localities. a. A map of the modern Asian monsoon system, the Tibetan Plateau and the position of Yunnan (Modified from An et al., 2006). b. The position of the study localities in Yunnan (DJ: Dajie coal mine, HX: Hexi coal mine, PJ: Pojiao coal mine, SG: Shanggang coal mine).

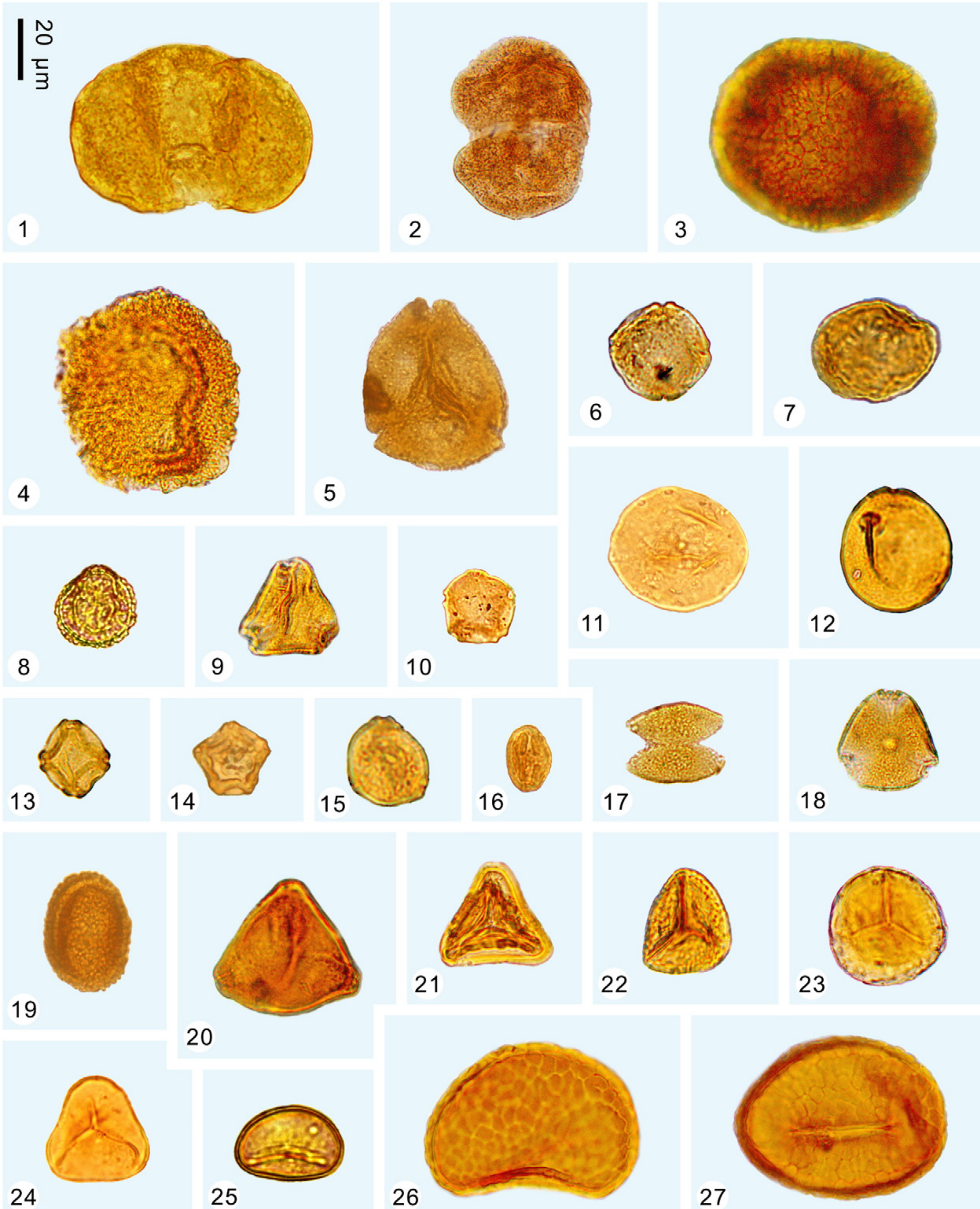

Fig. 3. A selection of the spores and pollen recovered from four locations (all palynomorphs are illustrated at the same magnification. Scale bar = 20 μm) 1–2. *Pinus*, 3–4. *Tsuga*, 5. Caprifoliaceae, 6–7. *Ulmus*, 8. Oleaceae, 9. Rhamnaceae, 10–11. *Juglans*, 12. *Carya*, 13–14. *Alnus*, 15. *Betula*, 16. *Castanopsis*, 17. Palmae, 18. Leguminosae, 19. Acanthaceae, 20. Elaeagnaceae, 21. *Pteris*, 22–23. Hymenophyllaceae, 24. Hemionitidaceae, 25. *Athyrium*, 26–27. Polypodiaceae.

No megathermic element appears in this zone. There are four mega-mesothermic elements (*Ilex*, *Castanopsis*, Myrtaceae and Anacardiaceae), seven mesothermic elements (e.g. *Alnus*, *Corylus*), two meso-microthermic elements (*Pinus* and *Tsuga*), and no microthermic element.

3.1.3. The PJ palynological assemblage

In the PJ coal mine, the 33 palynomorphs consist of 25 angiosperms (belonging to 22 families and accounting for 61.66% of the total number of pollen and spores), three gymnosperms (three families/1.05%) and five pteridophytes (five families/31.82%) (Table S3).

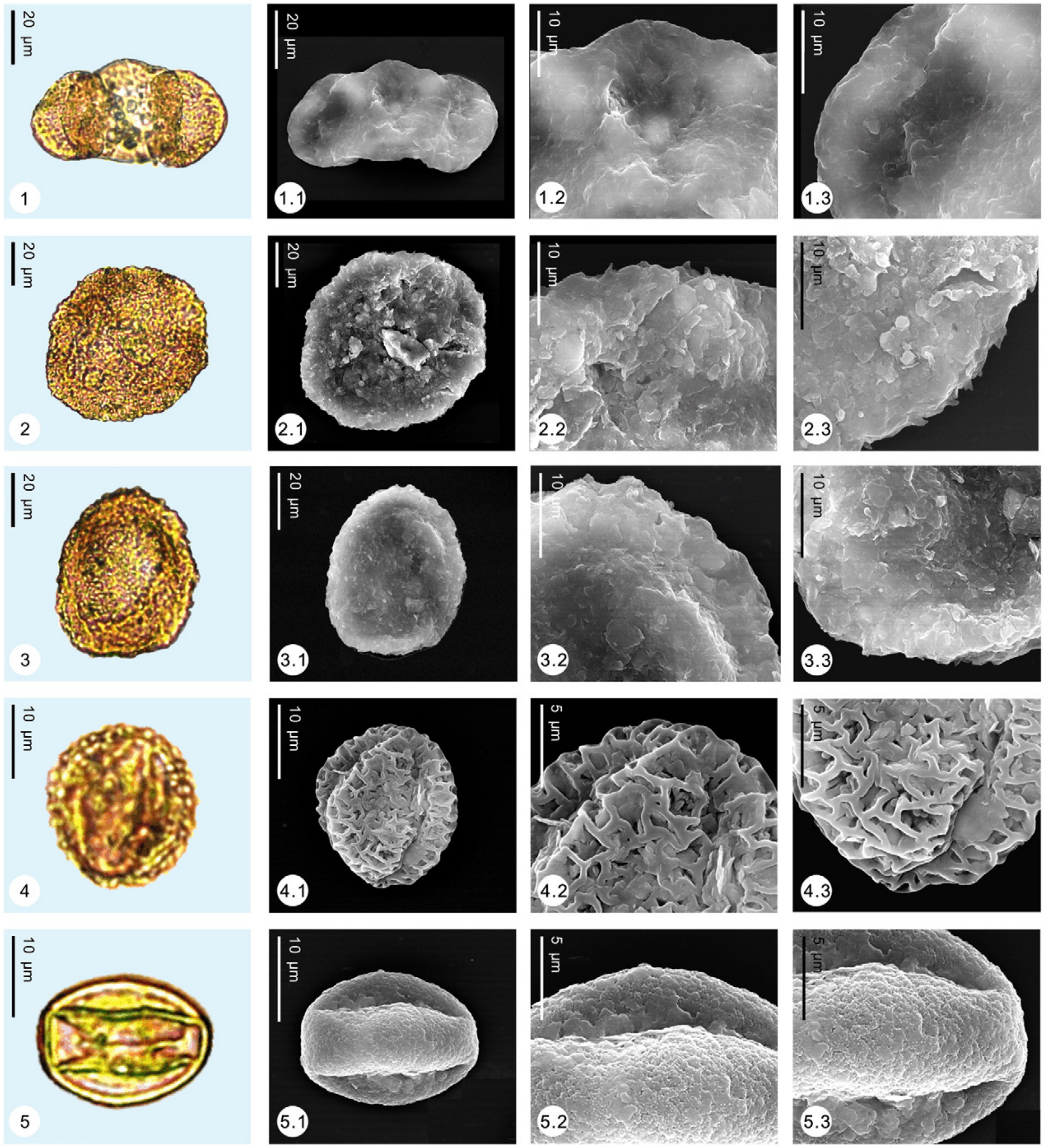

Fig. 4. 1. *Pinus* (1.2. shows details of the body; 1.3. shows details of airsac), 2–3. *Tsuga*, 4. Oleaceae, 5. *Quercus*.

One megathermic elements (Meliaceae), two mega-mesothermic elements (*Castanopsis* and Myrtaceae), nine mesothermic elements (e.g., *Betula*, *Corylus*), and two meso-microthermic elements (*Pinus* and *Tsuga*), are present. The microthermic elements are missing.

3.1.4. The SG palynological assemblage

In the SG coal mine, the 26 palynomorphs consist of 18 angiosperms (belonging to 12 families and accounting for 91.46% of the total number of pollen and spores), four gymnosperms (three families/3.49%) and four pteridophytes (four families/4.94%) (Table S4).

There are two megathermic elements (Rutaceae and Meliaceae), three mega-mesothermic elements (Taxodiaceae, *Castanopsis* and Anacardiaceae), 10 mesothermic elements (e.g., *Alnus*, *Juglans*), and two meso-microthermic elements (*Pinus* and *Tsuga*), while the microthermic elements are missing.

3.2. Palaeovegetation

The number of angiosperms, gymnosperms and pteridophytes taxa in these four localities (e.g., DJ, HX, PJ and SG) and their percentages of pollen/spores are shown in Fig. 7. Generally, the angiosperms were dominant in the four localities with a decrease in the number of taxa from 37 to 31 to 25 to 18 from north to south, but the percentages of angiosperm taxa in the palynofloras at each locality are not significantly different (63% at DDJ, 69% at HX, 76% at PJ and 69% at SG). In this case, an increase in the angiosperm pollen numbers

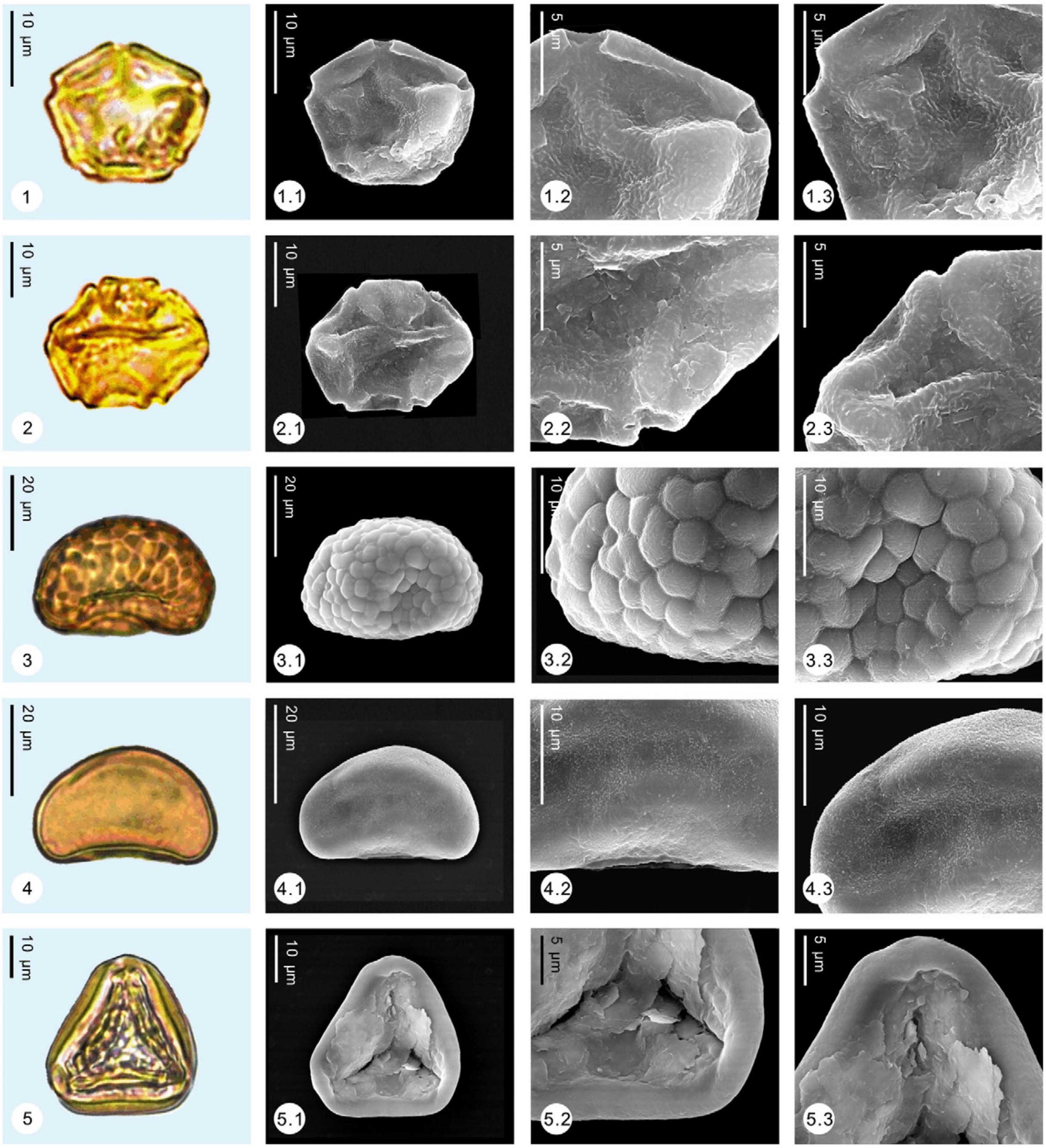

Fig. 5. 1,2. *Alnus*, 3. Polypodiaceae, 4. *Athyrium*, 5. *Pteris*.

from 30% to 46% to 61% to 92% from north to south may reflect the luxuriance of angiosperms in southern Yunnan growing under more congenial climatic conditions. *Alnus* was the major element of the deciduous broad-leaved forest, followed by *Betula*, *Corylus*, *Ulmus*, *Juglans*, *Castanea*, and *Carya*. *Castanopsis* represented the main element of the evergreen broad-leaved forest, followed by Palmae, Myrtaceae, Rutaceae, and Proteaceae. Although both *Alnus* and *Castanopsis* dominated the angiosperms in DJ, HX and SG, *Alnus* was missing at PJ.

The palynological assemblages suggest that the Middle Miocene vegetation of the four localities was composed of mixed evergreen and deciduous broad-leaved forests with some conifers growing under subtropical conditions. The vegetation in central and southern Yunnan in the Middle Miocene showed variations, based on the data obtained from this work on the four localities. The high percentages (approximately 9 to 12%) of coniferous pollen at DJ and HX may suggest the presence of zonal vegetation in the mountains surrounding these two localities. The evergreen broad-leaved forests with mega-mesothermic and megathermic elements are most likely to have occupied the valleys and basins. The deciduous broad-leaved forests with mesothermic elements most likely grew on the hillsides at low altitudes. The coniferous trees are likely to have occurred on the mountains at high altitudes (Fig. S1), as in recent Yunnan vegetation. The high density of the forests resulted in a shady undergrowth with a high humidity, which was conducive to the growth of ferns at DJ, HX and PJ. The coniferous pollen in PJ and SG was only present at low percentages (from 1 to 3.5%), and the pollen may have been transported there by wind. The altitude of the localities of PJ and SG may not have been as high as that of DJ and HX. As a result, the vertical vegetation zones there were less well-developed. The angiosperms

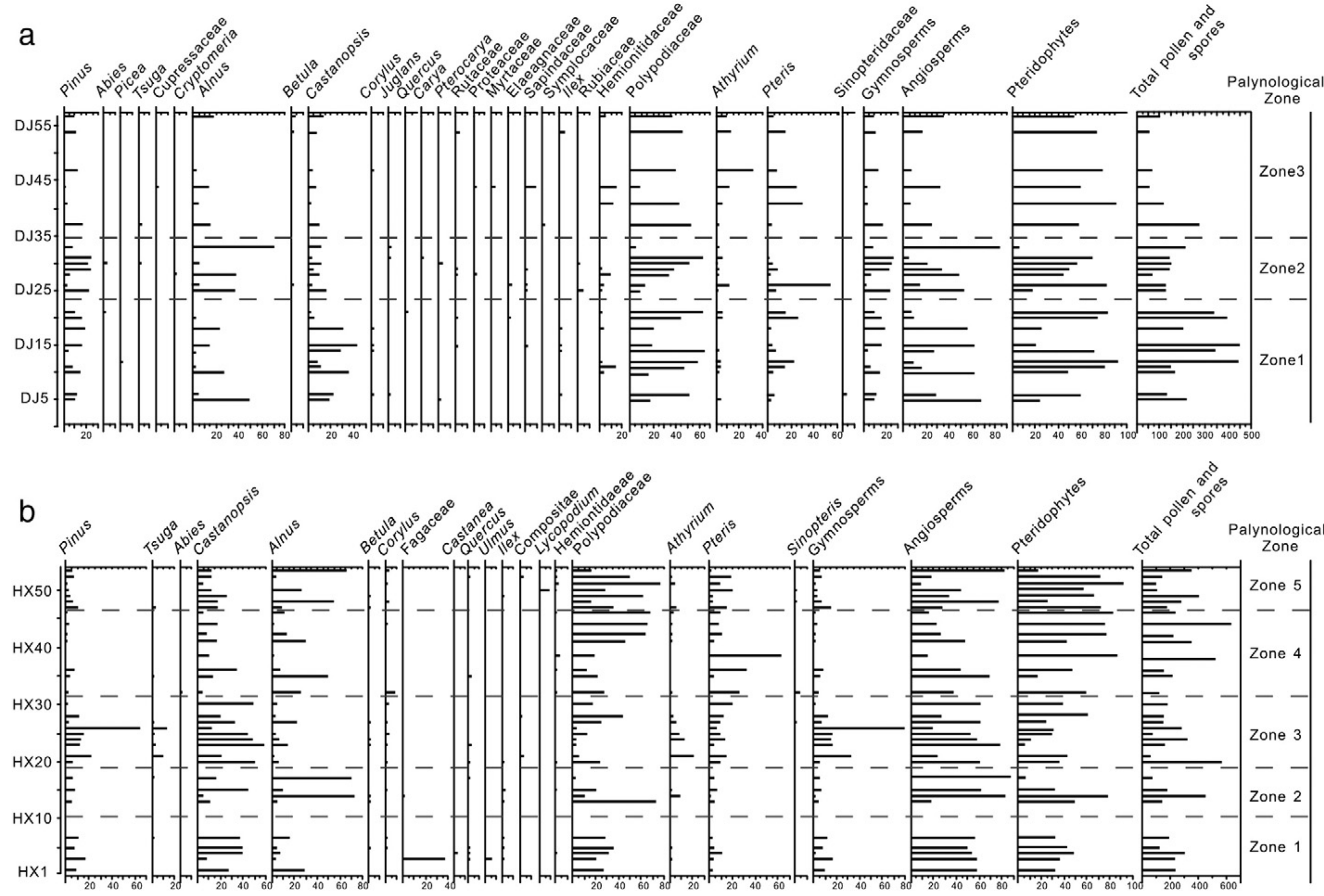

Fig. 6. The pollen diagrams showing the percentage values of the main taxa. a. The DJ section. b. The HX section.

dominated the vegetation at SG, while the evergreen and deciduous broad-leaved forests were widespread. The high percentage of *Alnus* pollen at SG may reflect its riparian habitat.

Because both mega-mesothermic and megathermic elements grew at these localities, the climate must have been somewhere from warm to hot in the four localities during the Middle Miocene. Xerophilous plants (*Ephedra*) were found at the four localities, which may suggest that there were dry habitats in some areas. Influenced by the topography, the local climate would have varied from warm-humid to warm-dry conditions in central and southern Yunnan in the Middle Miocene.

3.3. Palaeoclimate

By applying the CA, we obtained the climatic parameters for DJ, HX, PJ and SG.

3.3.1. The palaeoclimate at DJ

Based on the nearest living relatives (NLRs) of 45 spermatophytic taxa, we obtained the climatic parameters of the whole section of DJ (Fig. S2). They are MAT = 11.5 (delimited by Palmae)–17.3 °C (*Cryptomeria*); MWMT = 19.8 (*Carya*)–28.0 °C (Araliaceae); MCMT = −0.2 (Palmae)–5.9 °C (*Ephedra*); DT = 12.3 (*Picea*)–24.6 °C (Proteaceae); MAP = 793.9 (Palmae)–1389.4 mm (*Ephedra*); MMaP = 172.4 (Hamamelidaceae)–245.2 mm (*Ephedra*) and MMiP = 6.9 (*Carya*)–22.1 mm (*Pterocarya*). Compared with the modern meteorological data at Jingdong (Table 1), it is evident that the climate at DJ was colder in the Middle Miocene than today (MAT: 14.6 compared with (comp.) 18.3 °C; DT: 18.5 comp. 12.3 °C), with a slightly warmer summer (MWMT: 23.9 comp. 23.2 °C) but a much colder winter (MCMT: 2.9 comp. 10.9 °C).

We also obtained the seven climatic parameters of the three zones (Table S5). Considering the changes of climatic parameters in these three zones, it would seem that it was warmer in the periods of Zone 3 than in Zones 1 and 2, with approximately the same precipitation in all three zones and only a little more in Zone 2.

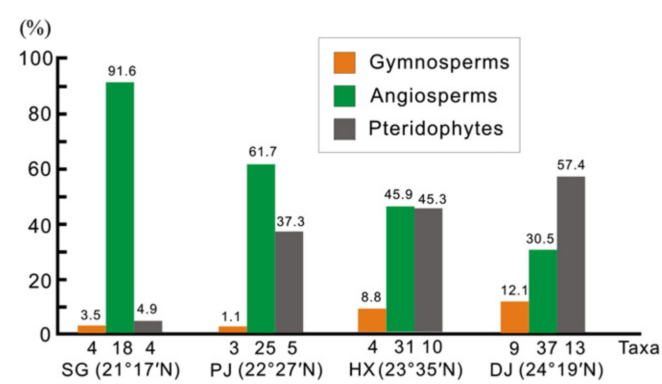

Fig. 7. The percentage values of angiosperms, gymnosperms and pteridophytes from the four coal mines.

Table 1
The comparison of the climatic parameters from the Middle Miocene of DJ, HX, PJ and SG, the Late Miocene of Lühe and Kaiyuan, the Late Pliocene of Eryuan, Yangyi and Longling, and the present-day of Jingdong, Zhenyuan, Simao and Mengla (▲—median value of the climatic parameters; ■—mean value of the climatic parameters).

Period	Location	Latitude and longitude	MAT	MWMT	MCMT	DT	MAP
			(°C)	(°C)	(°C)	(°C)	(mm)
Middle Miocene▲	DJ	23.25°N, 100.41°E[a]	14.4	23.9	2.9	18.5	1091.7
	HX	22.25°N, 99.63°E[a]	16.2	23.4	2.9	19.1	1091.7
	PJ	21.47°N, 100.84°E[a]	16.7	23.4	2.9	18.4	1091.7
	SG	20.29°N, 101.09°E[a]	16.7	23.6	2.9	19.1	1091.7
Late Miocene▲	Lühe	25°01′N, 101°32′E	17.1	25	7.6	18.5	1029.2
	Kaiyuan	23°48′N, 103°12′E	17.9	25.7	8.2		1427.0
Late Pliocene▲	Eryuan	26°00′N, 99°49′E	15.9	26.1	7	15.4	1052.1
	Yangyi	24°57′N, 99°15′E	17.1	25	7.3	19.1	1026.1
	Longling	24°41′N, 98°50′E	20.4	25.2	12.4	15.2	1035.2
Present ■	Jingdong	24°28′N, 101°05′E	18.3	23.2	10.9	12.3	1087.0
	Zhenyuan [b]	23°24′-24°22′N, 100°21′-101°31′E	19.1	23.5	12.5		1243.6
	Simao	22°40′N, 101°24′E	17.7	21.7	11.5	10.2	1522.6
	Mengla	21°29′N, 101°34′E	21.0	24.7	15.2	9.5	1540.2

[a] The palaeolatitude and palaeolongitude are obtained by using ARCGIS software.
[b] The Meteorological record of Zhenyuan comes from this website http://pesm.xxgk.yn.gov.cn/canton_model12/newsview.aspx?id=78766.

3.3.2. The palaeoclimate at HX

Based on 35 spermatophyte taxa, we procured the climatic parameters of the whole section of HX (Fig. S3). They are MAT = 11.5 (Palmae)–20.8 °C (*Tilia*); MWMT = 18.7 (Palmae)–28.0 °C (Araliaceae); MCMT = −0.2 (Palmae)–5.9 °C (*Ephedra*); DT = 12.1 (*Ephedra*)–26.0 °C (Palmae); MAP = 793.9 (Palmae)–1389.4 mm (*Ephedra*); MMaP = 172.4 (Hamamelidaceae)–245.2 mm (*Ephedra*) and MMiP = 5.7 (*Abies*)–22.1 mm (*Pterocarya*). By comparison with the modern meteorological data from Zhenyuan (Table 1), it is obvious that the climate at HX in the Middle Miocene was colder and drier than today (MAT: 13.2 comp.19.1 °C; MAP: 1091.7 comp. 1243.6 mm).

We also obtained the seven climatic parameters of the five zones (Table S5). Of these, only the climate in Zone 4 was warm and humid (MAT: 11.5 to 20.8 °C comp. 5.4/5.7 to 23.8 °C; MAP: 793.9 to 1389.4 comp. 613.8 to 1389.4 mm).

3.3.3. The palaeoclimate at PJ

Based on 28 spermatophytic taxa, we obtained the climatic parameters of the PJ section (Fig. S4, Table S5). They are MAT = 11.5 (Palmae)–21.9 °C (*Tsuga*); MWMT = 18.7 (Palmae)–28.0 °C (Araliaceae); MCMT = −0.2 (Palmae)–5.9 °C (*Ephedra*); DT = 12.1 (*Ephedra*)–24.6 °C (Proteaceae); MAP = 793.9 (Palmae)–1389.4 mm (*Ephedra*); MMaP = 139 (Proteaceae)–245.2 mm (*Ephedra*) and MMiP = 4.9 (Proteaceae)–23.6 mm (*Ephedra*). A comparison with the modern meteorological data from Simao (Table 1) suggests that the climate at PJ possessed a colder winter and a lower precipitation in the Middle Miocene than today (MCMT: 2.9 comp. 11.5 °C; MAP: 1091.7 comp. 1522.6 mm).

3.3.4. The palaeoclimate at SG

Based on 22 spermatophytic taxa, we obtained the climatic parameters of the SG section (Fig. S5, Table S5). They are MAT = 11.5 (Palmae)–21.9 °C (*Tsuga*); MWMT = 18.7 (Palmae)–28.5 °C (Gramineae); MCMT = −0.2 (Palmae)–5.9 °C (*Ephedra*); DT = 12.1 (*Ephedra*)–26.0 °C (Palmae); MAP = 793.9 (Palmae)–1389.4 mm (*Ephedra*); MMaP = 137.3 (*Castanopsis*)–245.2 mm (*Ephedra*) and MMiP = 4.5 (*Pterocarya*)–22.1 mm (*Pterocarya*). A comparison with the modern meteorological data from Mengla (Table 1), shows that it was colder and drier in the Middle Miocene than today at SG (MAT 13.2 comp. 21.0 °C; MAP 1091.7 comp. 1540.2 mm) and that it was more similar to the climates at HX and PJ.

4. Discussion

4.1. The Middle Miocene climate at the southeastern edge of the Tibetan Plateau

The climatic parameters obtained by the method of CA in this work demonstrate the similarity of the climates at all four localities. Except for the MAT, the parameters there possess very similar coexistences, i.e., MWMT from 18.7 to 28.5 °C, MCMT from −0.2 to 5.9 °C, DT from 12.1 to 26 °C, MAP from 793.9 to 1389.4 mm, MMaP from 137.3 to 245.2 mm and MMiP from 4.5 to 23.6 mm (Fig. S6). The minimum values (11.5 °C) of MAT at the four localities are the same, but the maximum value is lower (14.4 °C) at DJ than at the other three localities (16.2–16.7 °C). As a result, the median value of MAT is 1.8 °C lower at DJ (14.4 °C) than at HX and is 2.3 °C lower than at PJ and SG (16.7 °C).

The latitudinal difference between DJ (24°19′25.3″N) and SG (21°17′05.9″N) is approximately 3°. According to the latitudinal temperature gradient, which was approximately 0.3 °C per degree in the Early to Middle Miocene (J.F. Li et al., 2009), the temperature difference would be approximately 0.9 °C, i.e., the MAT should be 0.9 °C lower at DJ than at SG, whereas in fact it was 2.3 °C lower at DJ than at SG.

It appears that the uplift of the Ailao Mountains influenced the climate in the areas including PJ and SG in the Middle Miocene. A similar phenomenon is seen in Yunnan at the present day: Yuanmou Valley in Yuanmou County (25°42′N) is close to the Jinsa River and possesses an extremely hot and dry climate in the valley, with a MAT of 21.9 °C, whereas Jiangcheng City (22°31′N), Yunnan has a MAT of 18.1 °C (IDBMC, 1984). This is caused by a Foehn effect and results in the valley having tropical plants, such as palm and banana; however, on the slopes and on the top of the mountain there are temperate forests, as at Yuanmou today. The interaction of the uplift of mountains and the erosion of rivers in the Yunnan Plateau produced the dry–hot valleys over the course of time. The topography of the basins, mountains, and valleys influenced the local climates there, as at HX and PJ and SG.

In comparison with the present meteorological data from the southeastern edge of the Tibetan Plateau, it is evident that the climate was colder, with less precipitation in the Middle Miocene than today (Table 1).

Zachos et al. (2001) suggested that the temperature was higher in the Miocene than today as a result of global cooling during the Cenozoic. In contrast, in the study area the temperatures in the Miocene

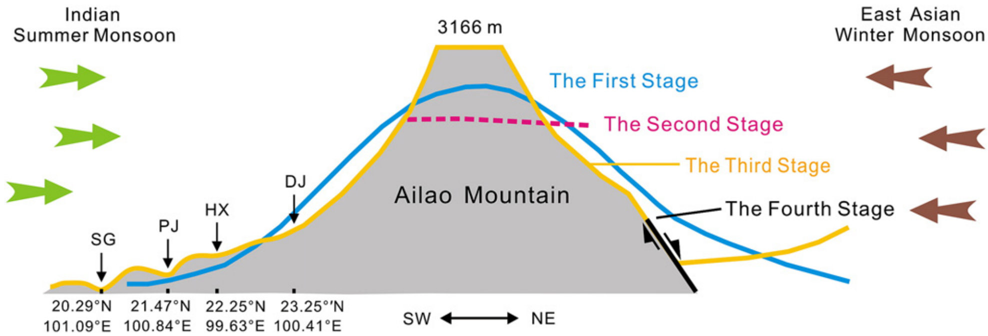

Fig. 8. The four stages of the evolution of the Ailao Mountains (according to Wang et al., 2006).

were lower than they are today. This observation raises a question regarding the cause of this phenomenon.

The uplift of Tibet influenced the topography and climate in East Asia, and especially changed the landscapes in southwestern China, including Yunnan, Sichuan and Guizhou; further, the uplift initiated the monsoon system in Asia (Li, 1999; An et al., 2001, 2006). During the Middle Miocene, the topography in Yunnan and the monsoonal system in East Asia had already developed to some degree (Li, 1999; An et al., 2001; Sun and Wang, 2005; An et al., 2006).

The areas studied in this paper are situated on the southwestern side of the Ailao Mountains (Fig. S7). The Ailao Mountain range is approximately 800 km long, and extends in a NW–SE direction, with an average elevation of over 2000 m with the highest peak 3166 m above sea level (Wang, 2002). The mountain range forms a natural boundary separating the eastern region and the southwestern region of the Yunnan Plateau, and the mountain range plays an important role in influencing the temperature and rainfall (Wang, 2002; Hao et al., 2009).

The Ailao Mountains have gone through four stages to attain their present altitudes (Wang et al., 2006) (Fig. 8). In the first stage, in the Early Miocene (approximately 22–17 Ma), orogenic movement caused the uplift of the Ailao Mountains. Second, in the late Early Miocene and the Middle Miocene (approximately 20–10 Ma), the mountains were eroded into a landform with low relief. In the third stage in the late Middle Miocene and the early Late Miocene (approximately 13–9 Ma), the landscape was changed by the regional uplift of the mountains, coevally with the incision of river systems. Finally, during the Late Cenozoic (approximately 5 Ma), the mountains were uplifted strongly.

It is presumed that the Ailao Mountains were not high enough to stop the winter monsoon or to reduce its influence on the southwestern slope of the mountains in the Middle Miocene. It is evident that the MCMTs in these areas were lower in the Middle Miocene than today (2.9 comp. 10.9–15.2 °C). It would seem that recently the high elevation of the Ailao Mountains either stops or reduces the winter monsoon and also causes the warm winter. For the same reason, the Ailao Mountains also block the moist airstream of the summer monsoon from the Indian Ocean, causing more rainfall to fall on the southwestern slope of the mountains today than in the Middle Miocene times (1087–1540 comp. 1092 mm). The other reason for the higher MAT today than in the Middle Miocene is that the summer monsoons were less intense (Li, 1999; An et al., 2001; Sun and Wang, 2005; An et al., 2006).

The uplift of the Ailao Mountains was caused by the tectonic movement of the neighbouring Tibetan Plateau. The uplift of the Tibetan Plateau changed the landscapes and climates of Yunnan considerably (Yang et al., 2010).

4.2. Comparison with the Middle Miocene vegetation and climate of the Tibetan Plateau

Two megathermic elements (Palmae and Meliaceae), two mega-mesothermic elements (*Castanopsis* and Myrtaceae), eight mesothermic elements (e.g., *Betula*, *Corylus*), and two meso-microthermic elements (*Pinus* and *Tsuga*), are present. The microthermic elements are missing.

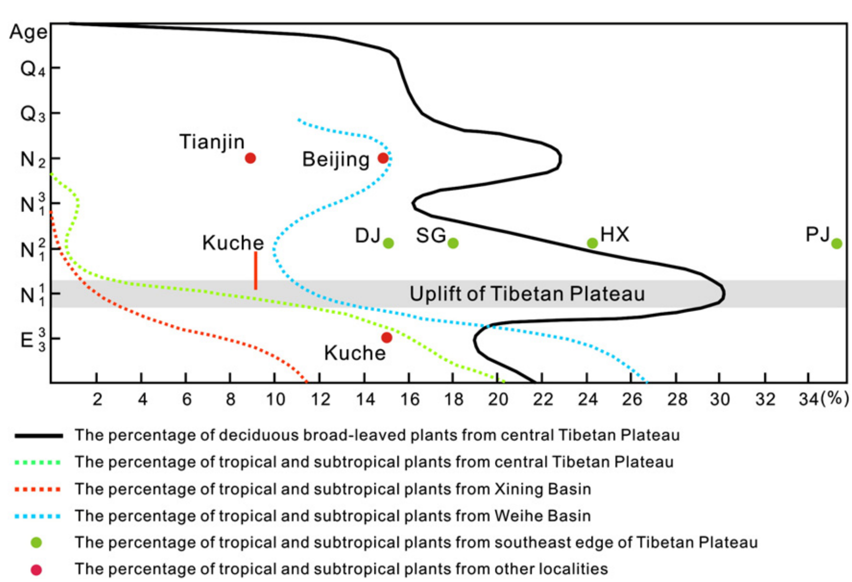

Fig. 9. The changes in the Late Cenozoic palynological assemblages of the Tibetan Plateau and the surrounding areas (Modified from Wu et al., 2006).

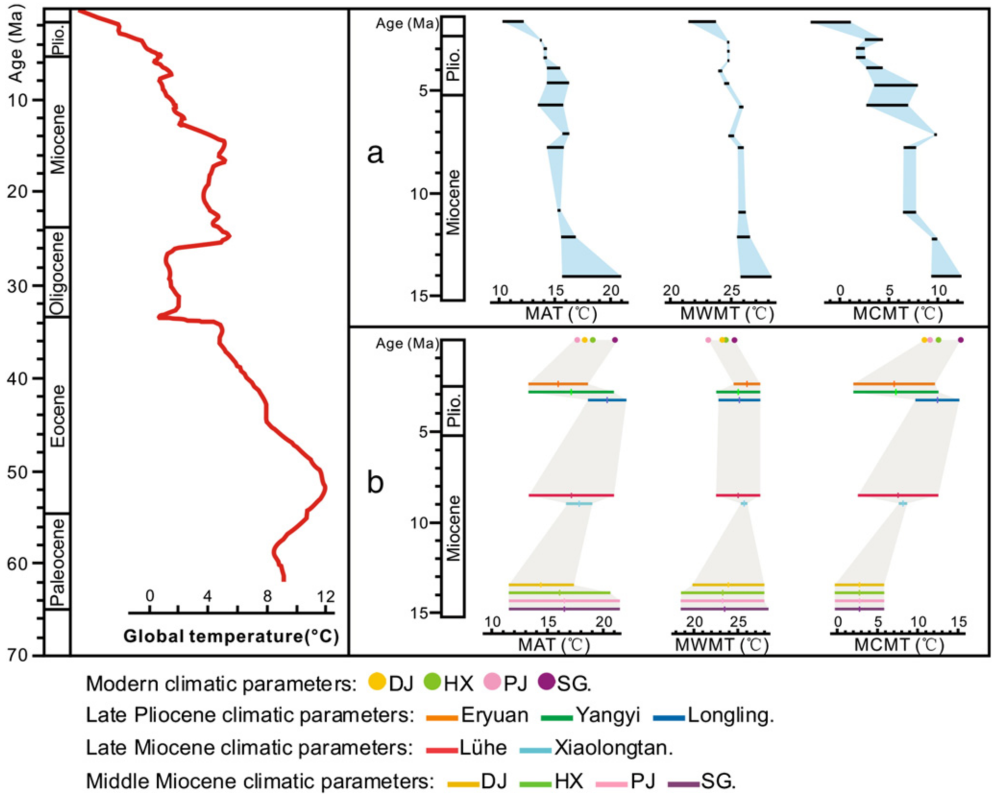

Fig. 10. The Neogene climatic comparison between SW China and Central Europe. The global temperature curve is modified from Zachos et al. (2001). a. The temperature curves for Central Europe (modified from Mosbrugger et al., 2005). b. The temperature curves for SW China.

The Middle Miocene climate of the Tibetan Plateau was inferred from reconstructing the palaeovegetation. Wu et al. (2006) reported pollen assemblages from the Nagqu Basin, in the central Tibetan Plateau of the Middle-Late Miocene age. This report suggested that the vegetation there was a needle- and broad-leaved mixed forest with various herbs growing in the understory. Megatherm and mega-mesotherm were hardly represented, while the conifers and herbs were increasing in abundance. Mesothermic and meso-microthermic trees such as *Pinus*, *Celtis* and *Quercus* were dominant. The most common herb was Chenopodiaceae, while aquatic and/or marsh plants were rare. The pollen assemblages indicate that a cool and dry climate prevailed on the central Tibetan Plateau in the Middle Miocene. Based on a further comparison (Wu et al., 2006), it is clear that the megatherm and mega-mesotherm of the Tibetan Plateau decreased sharply since the Early Miocene. For example, the megatherm and mega-mesotherm decreased from 3% to 5% (Early Miocene) to 0.5% (Middle Miocene) of the total numbers of pollen and spores in the Xining Basin and were also absent in the Late Miocene. The megatherm and mega-mesotherm decreased from 7% (Early Miocene) to 1% (Middle–Late Miocene) on the central Tibetan Plateau and disappeared there by the Pliocene. The megatherm and mega-mesotherm were replaced by needle- and temperate broad-leaved trees. However, the megatherm and mega-mesotherm were still living in the area surrounding the Tibetan Plateau during the Neogene. For example, the megatherm and mega-mesotherm increased from 10% to 12% in the Miocene to 15% in the Pliocene of the Weihe Basin, and 15% in Beijing, and 9% in Tianjin in the Pliocene (Fig. 9).

According to our study, the Middle Miocene vegetation at the southeastern edge of the Tibetan Plateau had megathermic/mega-mesothermic elements (e.g., Palmae, Rutaceae, Meliaceae and *Castanopsis*) and hygrophilous elements (e.g., *Alnus* and Taxodiaceae). The percentage of megatherm and mega-mesotherm (DJ: 14.84%, HX: 24.06%, PJ: 35.48%, SG: 18.00% of the total number of pollen and spores) was much higher than on the central Tibetan Plateau (1%) (Fig. 6), which suggests that the Middle Miocene climate at the southeastern edge of the Tibetan Plateau was warmer and wetter than that of the plateau itself. This phenomenon could be caused by the strong uplift of the mountains of the central Tibetan Plateau.

The opinions on the elevations of the Tibetan Plateau in the Middle Miocene differ strongly. Some researchers suggest that the Tibetan Plateau was not uplifted to its present altitude in the Middle Miocene (Li, 1999; An et al., 2001; Jia et al., 2004; An et al., 2006), while other investigations have suggested that the southern Tibetan Plateau has not significantly changed in elevation since the Middle Miocene era (Spicer et al., 2003; Song et al., 2010). However, both factions believe that the Tibetan Plateau was uplifted in the Middle Miocene. Based on the pollen evidence, the elevation of the Tibetan Plateau in the Miocene was approximately 3000–3150 m (Song et al., 2010). On the other hand, the southeastern edge of the Tibetan Plateau was uplifted strongly and successively during the last 1.4 Ma (Yang et al., 2010). This has been confirmed by a comparison of the vegetation between the central Tibetan Plateau and the southeastern edge of the plateau.

4.3. Neogene climatic changes at the southeastern edge of the Tibetan Plateau and a comparison with Central Europe

The new parameters were compared with the climatic data from Lühe and Xiaolongtan (Late Miocene) (Xu et al., 2008; Xia et al., 2009), Eryuan, Yangyi and Longling (Late Pliocene) (Kou et al., 2006) and Jingdong, Zhenyuan, Simao and Mengla at present (IDBMC, 1984) (Table 1). In this way, the temperature curves of the southeastern edge of the Tibetan Plateau were obtained (Fig. 10b).

A comparison with the global marine temperature record (Zachos et al., 2001) and the climate of Central Europe (Mosbrugger et al., 2005) (Fig. 10a) reveals that: 1) in contrast to the Neogene cooling (Zachos et al., 2001; Mosbrugger et al., 2005), the MAT curve of the southeastern edge of the Tibetan Plateau exhibited a general warming trend. In Yunnan, the MAT from the Middle Miocene to the Late

Miocene to the Late Pliocene to today increased (13.2–14.6 comp. 17.1–17.9 comp. 15.9-20.4 comp. 17.7–21 °C) (Table 1). 2) The MWMT curves of the southeastern edge of the Tibetan Plateau and Central Europe did not change significantly after the Middle Miocene. 3) The MCMT curves from the southeastern edge of the Tibetan Plateau and Central Europe display different trends. The MCMT values increased markedly since the Middle Miocene on the southeastern edge of the Tibetan Plateau, while they decreased in Central Europe.

The climate at the southeastern edge of the Tibetan Plateau gradually warmed over the course of 15 million years. The change in MAT is in apparent contradiction to the climatic changes of Central Europe, although in accordance with the climatic changes of Northern Australia. According to Kershaw and Wagstaff (2001), Northern Australia shows an increasing temperature from the Miocene as a result of its movements into the tropical latitudes. In Yunnan, the palaeolatitude and palaeolongitude hardly changed following the Middle Miocene (Table 1). The climate warming trend in Yunnan (southeastern edge of the Tibetan Plateau) appears to be linked to the successive uplift of the Tibetan Plateau, which eventually created an effective barrier to the Asian Winter Monsoon.

The uplift of the Tibetan Plateau, which caused the uplift of the Yunnan Plateau and created the complex topography in Yunnan (Yang et al., 2010), influenced the climatic changes in Yunnan during the Neogene. It resulted in the warmer conditions observed in Yunnan today.

5. Conclusions

The comprehensive palaeovegetational and palaeoclimatic studies of the pollen samples from the Dajie Formation in Yunnan, at the southeastern edge of the Tibetan Plateau, lead to the following conclusions:

1. The vegetation in Yunnan in the Middle Miocene era was composed of mixed evergreen and deciduous broad-leaved forests with some conifers.
2. The Middle Miocene vegetation in Yunnan suggests a subtropical climate.
3. The Middle Miocene climate in Yunnan was obviously cooler than today. It suggests that the Ailao Mountains were not high enough to block the Asian Winter Monsoon in the Middle Miocene.
4. The Middle Miocene vegetation at the southeastern edge of the Tibetan Plateau was compared with that of the central Tibetan Plateau. It appears that the palaeoclimate at the southeastern edge of the plateau was warmer and wetter than in central Tibet.
5. In contrast to the Neogene cooling in Central Europe, the climate around the southeastern edge of the Tibetan Plateau became gradually warmer since the Middle Miocene, with increases in MAT and MCMT. The increase of MCMT might signal the weakening of the winter monsoon. This phenomenon was most likely caused by the uplift of the Tibetan Plateau, which has succeeded in blocking the Asian Winter Monsoon since the Middle Miocene.

Acknowledgements

The authors would like to thank Senior Engineer Nai-Qiu Du at the Institute of Botany, CAS, Beijing, China, for her help with pollen identifications. We are also grateful to Mr. Julien Cillis at the Royal Belgian Institute of Natural Sciences, Brussels, Belgium, for his technical assistance with SEM, and Dr. Nilamber Awasthi, Ex-Deputy Director at the Birbal Sahni Institute of Palaeobotany, Lucknow, India, for his useful suggestions on the manuscript. This research was supported by the International S & T Cooperation Project of China No. 2009DFA32210, the program of the Natural Science Foundation of China (NSFC) No. 41072022, No. 41210001, the key program of NSFC No. 30530050 and the National Basic Research Program of China (2004CB720205).

Appendix A. Supplementary data

Supplementary data to this article can be found online at http://dx.doi.org/10.1016/j.palaeo.2012.08.009.

References

An, Z.S., Kutzbach, J.E., Prell, W.L., Porter, S.C., 2001. Evolution of Asian monsoons and phased uplift of the Himalaya-Tibetan plateau since Late Miocene times. Nature 411, 62–66.

An, Z.S., Zhang, P.Z., Wang, E.Q., Wang, S.M., Qian, X.K., Li, L., et al., 2006. Changes of the monsoon-arid environment in China and growth of the Tibetan Plateau since the Miocene. Quaternary Science 26, 678–693 (in Chinese with English abstract).

BGMRYP (Bureau of Geology and Mineral Resources of Yunnan Province), 1990. Regional Geology of Yunnan Province. Geological Publishing House, Beijing, pp. 1–728 (in Chinese).

Böhme, M., Bruch, A.A., Selmeier, A., 2007. The reconstruction of Early and Middle Miocene climate and vegetation in Southern Germany as determined from the fossil wood flora. Palaeogeography, Palaeoclimatology, Palaeoecology 253, 91–114.

Colani, M., 1920. Etude sur les flores Tertiaires de quelques gisements de lignite de 1'Indochine et du Yunnan. Bulletin du Service Géologique de l'Indochine 8, 1–609.

Dai, J., Sun, B.N., Xie, S.P., Wu, J.Y., Li, N., 2009. *Carpinus miofangiana* from the Pliocene of Tengchong in Yunnan Province and Its Palaeoclimatic Significance. Advanced Earth Sciences 24, 1024–1032.

Ferguson, D.K., Zetter, R., Paudayal, K.N., 2007. The need for the SEM in palaeopalynology. Comptes Rendus Palevol 6, 423–430.

Ge, H.R., Li, D.Y., 1999. Cenozoic Coal—Bearing Basins and Coal—Forming Regularity in West Yunnan. Yunnan Sci. Technol. Press, Kunming . (in Chinese with English summary).

Hao, C.Y., Chen, Z.C., Wu, S.H., 2009. Floristic elements of sediment spore-pollen between western and eastern sample plots beside main peak of Ailao Mountain in Yunnan. Subtropical Plant Science 38, 1–5.

Hao, H., Ferguson, D.K., Feng, G.P., Ablaev, A., Wang, Y.F., Li, C.S., 2010. Early Palaeocene vegetation and climate in Jiayin, NE China. Climatic Change 99, 547–566.

Hou, S.G., Li, J., 1993. Sporopollen assemblages in peat-lignite of Baoxiu basin, Yunnan. Coal Geology and Exploration 21, 15–18 (in Chinese with English abstract).

IBCAS (Institute of Botany, the Chinese Academy of Sciences), 1976. Sporae Pteridophytorum Sinicorum. Sci. Press, Beijing . (in Chinese).

IBCAS, SCIBCAS (Institute of Botany & South China Institute of Botany, the Chinese Academy of Sciences), 1982. Angiosperm Pollen Flora of Tropic and Subtropic China. Sci. Press, Beijing . (in Chinese).

IDBMC (Information Department of Beijing Meteorological Center), 1984. Land climate data of China (1951–1980) (part I - VI). China Meteorol. Press, Beijing . (in Chinese).

Jia, C.Z., He, D.F., Lu, H.M., 2004. Episodes and geodynamic setting of Himalayan movement in China. Oil & Gas Geology 25, 121–125 (in Chinese with English abstract).

Jiménez-Moreno, G., 2006. Progressive substitution of a subtropical forest for a temperate one during the middle Miocene climate cooling in Central Europe according to palynological data from cores Tengelic-2 and Hidas-53 (Pannonian Basin, Hungary). Review of Palaeobotany and Palynology 142, 1–14.

Kershaw, A.P., Wagstaff, B., 2001. The southern conifer family Araucariaceae: history, status, and value for paleoenvironmental reconstruction. Annual Review of Ecology and Systematics 32, 397–414.

Kershaw, A.P., van der Kaars, S., Flenley, J.R., 2007. The Quaternary history of Far Eastern rainforests. In: Bush, M.B., Flenley, J.R. (Eds.), Tropical Rainforest Responses to Climatic Change. Praxis Publishing Ltd, Chichester, pp. 77–115.

Kou, X.Y., Ferguson, D.K., Xu, J.X., Wang, Y.F., Li, C.S., 2006. The reconstruction of paleovegetation and paleoclimate in the Late Pliocene of west Yunnan, China. Climatic Change 77, 431–448.

Li, J.J., 1999. Studies on the geomorphological evolution of the Qinghai-Xizang (Tibetan) plateau and Asian monsoon. Marine Geology & Quaternary Geology 19, 1–11 (in Chinese with English abstract).

Li, X.Q., Du, N.Q., 1999. The acid–alkali-free analysis of Quaternary pollen. Acta Botanica Sinica 41, 782–784 (in Chinese with English abstract).

Li, J.J., Fang, X.M., 1998. Researches of Tibetan Plateau uplift and environmental changes. Chinese Science Bulletin 43, 1569–1574 (in Chinese).

Li, W.Y., Wu, X.F., 1978. A palynological investigation on the late Tertiary and early Quaternary and its significance in the paleogeographical study in Central Yunnan. Acta Geographica Sinica 33, 142–155 (in Chinese with English abstract).

Li, J.F., Ferguson, D.K., Yang, J., Feng, G.P., Ablaev, A.G., Wang, Y.F., Li, C.S., 2009. Early Miocene vegetation and climate in Weichang District, North China. Palaeogeography, Palaeoclimatology, Palaeoecology 280, 47–63.

Li, N., Sun, B.N., Wu, J.Y., Yan, D.F., Xiao, L., Dai, J., 2009. Cuticular structure of *Quercus presenescens* from the Pliocene in Baoshan, Yunnan, and its palaeoclimatic implications. Acta Palaeontologica Sinica 48, 654–661 (in Chinese with English abstract).

Liang, M.M., Bruch, A.A., Collinson, M.E., Mosbrugger, V., Li, C.S., Sun, Q.G., Hilton, J., 2003. Testing the climatic estimates from different palaeobotanical methods: an example from the Middle Miocene Shanwang flora of China. Palaeogeography, Palaeoclimatology, Palaeoecology 198, 279–301.

Moore, P.D., Webb, J.A., Collinson, M.E., 1991. Pollen analysis, second ed. Blackwell scientific publications, Oxford.

Mosbrugger, V., Utescher, T., 1997. The coexistence approach—a method for quantitative reconstruction of Tertiary terrestrial palaeoclimate data using plant fossils. Palaeogeography, Palaeoclimatology, Palaeoecology 134, 61–86.

Mosbrugger, V., Utescher, T., Dilcher, D.L., 2005. Cenozoic continental climate evolution of Central Europe. Proceedings of the National Academy of Sciences of the United States of America 102, 14964–14969.

Mulch, A., Chamberlain, C.P., 2006. The rise and growth of Tibet. Nature 439, 670–671.

Qin, F., Ferguson, D.K., Zetter, R., Wang, Y.F., Syabryaj, S., Li, J.F., Yang, J., Li, C.S., 2011. Late Pliocene vegetation and climate of Zhangcun region, Shanxi, North China. Global Change Biology 17, 1850–1870.

Retallack, G.J., 2007. Cenozoic paleoclimate on land in North America. Journal of Geology 115, 271–294.

Song, Z.C., 1988. Late Cenozoic palyno-flora from Zhaotong, Yunnan. Memoirs of Nanjing Institute of Geology and Palaeontology, Academia Sinica 24, 1–41 (in Chinese with English abstract).

Song, Z.C., Li, M.Y., 1976. Spore-pollen assemblages of Lufeng and Mouding in the early Upper Cretaceous and of Mengla in the late Upper Cretaceous–Paleogene. Cenozoic Fossils of Yunnan Province. Science Press, Beijing, pp. 9–56 (in Chinese).

Song, Z.C., Zhong, B.Z., 1984. Tertiary sporo-pollen assemblages from Jinggu, Yunnan. Bulletin of Nanjing Institute of Geology and Palaeontology, Academia Sinica 8, 1–41 (in Chinese with English abstract).

Song, X.Y., Spicer, R.A., Yang, J., Yao, Y.F., Li, C.S., 2010. Pollen evidence for an Eocene to Miocene elevation of central southern Tibet predating the rise of the High Himalaya. Palaeogeography, Palaeoclimatology, Palaeoecology 297, 159–168.

Spicer, R.A., Harris, N.B.W., Widdowson, M., Herman, A.B., Guo, S.X., Valdes, P.J., Wolfe, J.A., Kelley, S.P., 2003. Constant elevation of southern Tibet over the past 15 million years. Nature 421, 622–624.

Sun, X.J., Wang, P.X., 2005. How old is the Asian monsoon system? Palaeobotanical records from China. Palaeogeography, Palaeoclimatology, Palaeoecology 222, 181–222.

Sun, X.J., Wu, Y.S., 1980. Paleoenvironment during the time of *Ramapithecus lufengensis*. Vertebrata Palasiatica 18, 247–255 (in Chinese with English abstract).

Sun, B.N., Cong, P.Y., Yan, D.F., Xie, S.P., 2003. Cuticular structure of two angiosperm fossils in Neogene from Tengchong, Yunnan Province and its palaeoenvironmental significance. Acta Palaeontologica Sinica 42, 216–222 (in Chinese with English abstract).

Tao, J.R., 1986. Neogene flora of Lanping and its significance in middle watershed of Selween–Mekong–Yangtze Rivers. In: Chinese Academy of Sciences (Ed.), Comprehensive Scientific Expedition to the Qinghai-Xizang Plateau, vol. 2. Beijing Sci. Technol. Press, Beijing, pp. 58–65 (in Chinese with English abstract).

Tao, J.R., Chen, M.H., 1983. Neogene flora of south part of the waterland of Selween–Mekong–Yangtze Rivers (The Lin Cang Region), Yunnan. In: Chinese Academy of Sciences (Ed.), Comprehensive Scientific Expedition to the Qinghai-Xizang Plateau, vol. 1. Yunnan People's Press, Kunming, pp. 74–89 (in Chinese with English abstract).

Tao, J.R., Du, N.Q., 1982. Neogene flora Tengchong Basin in western the Himalayan–Tibetan region: constraints from ODP site 758, Yunnan, China. Acta Botanica Sinica 24, 273–281 (in Chinese with English abstract).

Tao, J.R., Kong, Z.C., 1973. The fossil florule and sporo-pollen assemblage of Shang-in coal series of Eryuan, Yunnan. Acta Botanica Sinica 15, 120–126 (in Chinese with English abstract).

Uhl, D., Klotz, S., Traiser, C., Thiel, C., Utescher, T., Kowalski, E., Dilcher, D.L., 2007. Cenozoic paleotemperatures and leaf physiognomy—a European perspective. Palaeogeography, Palaeoclimatology, Palaeoecology 248, 24–31.

Utescher, T., Mosbrugger, V., Ivanov, D., Dilcher, D.L., 2009. Present-day climate equivalents of European Cenozoic climates. Earth and Planetary Science Letters 284, 544–552.

Wang, W.M., 1996. A palynological survey of Neogene strata in Xiaolongtan Basin, Yunnan Province of South China. Acta Botanica Sinica 38, 734–748 (in Chinese with English abstract).

Wang, S.Y., 2002. Geography of Yunnan Province. Yunnan Ethical Press, Kunming, pp. 46–48 (in Chinese).

Wang, W.M., Shu, J.W., 2004. Late Cenozoic palynofloras from Qujing Basin, Yunnan, China. Acta Palaeontologica Sinica 43, 254–261 (in Chinese with English abstract).

Wang, F.X., Qian, N.F., Zhang, Y.L., Yang, H.Q., 1995. Pollen Flora of China, second ed. Sci. Press, Beijing . (in Chinese).

Wang, E.Q., Fan, C., Wang, G., Shi, X.H., Chen, L.Z., Chen, Z.L., 2006. Deformational and geomorphic processes in the formation of the Ailao shan–Dianchang range, west Yunnan. Quaternary Science 26, 220–227 (in Chinese with English abstract).

WGCPC (Writing Group of Cenozoic Plants of China), 1978. Cenozoic Plants from China, Fossil Plants of China, vol. 3. Sci. Press, Beijing, pp. 183–185 (in Chinese).

Wolfe, J.A., 1994. Tertiary climatic changes at middle latitudes of western North America. Palaeogeography, Palaeoclimatology, Palaeoecology 108, 195–205.

Wolfe, J.A., 1995. Paleoclimatic estimate from Tertiary leaf assemblages. Annual Review of Earth and Planetary Sciences 23, 119–142.

Wu, Z.Y., Ding, T.Y., 1999. Seed Plants of Yunnan. China. Sci. Technol. Press, Kunming . (in Chinese).

Wu, Z.H., Wu, Z.H., Ye, P.S., Hu, D.G., Peng, H., 2006. Late Cenozoic environmental evolution of the Qinghai–Tibet Plateau as indicated by the evolution of sporopollen assemblages. Geology in China 33, 966–979.

Xia, K., Su, T., Liu, Y.S., Xing, Y.W., Jacques, F.M.B., Zhou, Z.K., 2009. Quantitative climate reconstructions of the late Miocene Xiaolongtan megaflora from Yunnan, southwest China. Palaeogeography, Palaeoclimatology, Palaeoecology 276, 80–86.

Xu, J.X., Wang, Y.F., Du, N.Q., 2003. Late Pliocene vegetation and paleoclimate of Yangyi and Longling of West Yunnan province. Journal of Palaeogeography 5, 217–223 (in Chinese with English abstract).

Xu, J.X., Ferguson, D.K., Li, C.S., Wang, Y.F., 2008. Late Miocene vegetation and climate of the Lühe region in Yunnan, southwestern China. Review of Palaeobotany and Palynology 148, 36–59.

Yang, J., Wang, Y.F., Sun, Q.G., Li, C.S., 2002. Quantitative studies on paleoelevation and paleoclimate of Shanwang Miocene basin, east China. Earth Science Frontiers 9, 183–188 (in Chinese with English abstract).

Yang, D.Y., Li, L.P., Huang, D., Ge, Z.S., Xu, Q.M., Li, X.S., Han, Z.Y., 2010. Uplift characteristics of the Yunnan Plateau. Quaternary Science 30, 864–871.

Zachos, L., Pagani, M., Sloan, L., Thomas, E., Billups, K., 2001. Trends, rhythms, and aberrations in global climate 65 Ma to present. Science 292, 686–693.

Zhang, Y.L., Xi, Y.Z., Zhang, J.T., Gao, G.Z., Du, N.Q., Sun, X.J., Kong, Z.C., 1976. Sporae Pteridophytorum Sinicorum. Sci. Press, Beijing . (in Chinese).

Zhang, X.J., He, K.Z., Zhou, Z.G., 1996. Features of sporo-pollen assemblages and environment changes of Neogene in area of western Yunnan. Geoscience 10, 187–201 (in Chinese with English abstract).

Zhang, R.Z., Zheng, D., Yang, Q.Y., Liu, Y.H., 1997. Physical Geography of Hengduan Mountains. Sci. Press, Beijing . (in Chinese with English abstract).

Zhao, L.C., Wang, Y.F., Liu, C.J., Li, C.S., 2004. Climatic implications of fruit and seed assemblage from Miocene of Yunnan, southwestern China. Quaternary International 117, 81–89.

Zheng, S.Y., Sang, H.S., Liu, C.F., 1976. The estimate report of Puwen coal mine, Jinghong City, Yunnan Province. , pp. 1–10 (in Chinese, the Report of the Sixteenth Geological Survey Team, Yunnan Geological Survey).